文章编号:2095-6134(2022)02-0193-08

Ab initio simulations of NO adsorption on hematite (0001) surface: PBE versus PBE+U*

WU Cuixia[1], SUN Tao[1†], FABRIS Stefano[2], DU Lin[3]

(1 *College of Earth and Planetary Sciences, University of Chinese Academy of Sciences, Beijing* 100049, *China*;
2 *CNR-IOM DEMOCRITOS, Istituto Officina dei Materiali, Consiglio Nazionale delle Ricerche, Trieste* 34136, *Italy*;
3 *Environment Research Institute, Shandong University, Qingdao* 266237, *Shandong, China*)

(Received 24 July 2020; Revised 10 August 2020)

Wu C X, Sun T, FABRIS S, et al. Ab initio simulations of NO adsorption on hematite (0001) surface: PBE versus PBE+U[J]. Journal of University of Chinese Academy of Sciences, 2022, 39(2): 193-200. DOI: 10.7523/j.ucas.2020.0041.

Abstract NO_x ($x=1,2$) are major air-pollutants detrimental to human health and much effort has been devoted to find efficient photocatalysts capable of removing NO_x from air (de-NO_x). Recent experiments indicate that hematite (α-Fe_2O_3) is a promising de-NO_x photocatalyst. However some key features of the NO adsorption on the hematite surface remain unclear, hindering further comprehension of the photocatalytic process. Here we study the adsorption of NO on the hematite (0001) surface using the PBE+U method with a dispersion correction (vdw) in the framework of density functional theory (DFT). We find the addition of a Hubbard U term in the DFT Hamiltonian strongly affects the adsorption properties, with the adsorption energy (−0.64 eV) decreased by 50% with respect to those of PBE (−1.31 eV). This decrease is attributed to two factors: (i) the U term shifts the energy of Fe 3d orbitals away from the valence band maximum, making them chemically less active; (ii) the NO molecule has an unpaired π^* electron and is more sensitive to the electronic structure of the substrate. In contrast to the inclusion of U, the dispersion correction causes little change to the adsorption properties except increases the adsorption energy by about −0.18 eV. We use the Langmuir formula to calculate the thermal equilibrium coverage of NO on the hematite (0001) surface and find predictions made with the PBE+U vdw are more consistent with experiments. These results highlight the importance of strong electronic correlations in describing the hematite surface reactions, and may serve as a starting point to unravel the complete photocatalytic mechanism.

Keywords hematite; NO; photocatalysis; Langmuir; air pollution

CLC number: P578.4; X513 **Document code**: A **DOI**: 10.7523/j.ucas.2020.0041

NO 在赤铁矿(0001)表面吸附的第一性原理计算

吴翠霞[1], 孙涛[1], FABRIS Stefano[2], 杜林[3]

* Supported by National Natural Science Foundation of China (41972044, 91644214) and Strategic Priority Research Program (B) of Chinese Academy of Sciences (XDB18000000)

† Corresponding author, E-mail: tsun@ucas.ac.cn

（1 中国科学院大学地球与行星科学学院，北京 100049；2 意大利国家研究理事会材料研究所，的里雅斯特 34136；
3 山东大学环境研究院，山东 青岛 266237）

摘 要 氮氧化物 NO_x（NO，NO_2）是对人类健康有严重危害的大气污染物。近年来研究表明赤铁矿（α-Fe_2O_3）可作为高效光催化剂去除大气中 NO_x，但 NO_x 气体在赤铁矿表面的吸附特性还未明确，阻碍了对其催化机理的进一步认识。基于密度泛函理论，采用包括电子强关联效应的 PBE+U 以及色散力修正的方法，对 NO 气体分子在 α-Fe_2O_3（0001）晶面的吸附行为进行深入研究，发现基于 PBE+U 方法获得的吸附能（E_{ad} = −0.64 eV）比 PBE 获得的 E_{ad}（−1.31 eV）低近 50%。这是由于电子强关联项 U 的引入降低了表面铁原子 d 轨道对价带顶的贡献，抑制了其化学活性，而 NO 具有一个未成对的 π^* 轨道电子，使得其对吸附基体的电子结构格外敏感。与+U 不同，色散力修正不会显著改变体系的电子结构，只是使 E_{ad} 略有增加（−0.18 eV）。采用统计力学的 Langmuir 公式计算 NO 在 α-Fe_2O_3（0001）表面的热力学平衡占据数，发现基于+U 的吸附能得到的平衡占据数与实验观测更为一致。这些结果揭示了电子强关联效应在 α-Fe_2O_3 表面化学中的重要作用，并为进一步研究 NO_x 在 α-Fe_2O_3 表面的光催化反应机理奠定了基础。

关键词 三氧化二铁；一氧化氮；光催化；Langmuir；大气污染

NO_x（x=1, 2）are major air pollutants in urban areas originated from fossil fuel combustions in vehicles and power stations[1-2]. They are detrimental to human health and much effort has been devoted to remove them from air (de-NO_x). Among the various de-NO_x technologies under development, photocatalytic oxidation (PCO) is one of the most promising routines[3-4]: under sunlight, a photocatalytic substrate captures NO_x in the air and transforms them into non-volatile nitrates. These nitrates can then be rinsed away and the substrate regains its photocatalytic ability. So far the most common photocatalytic de-NO_x material is TiO_2, with TiO_2-based air purification devices being deployed in several European cities[4]. However due to its relatively large band-gap, TiO_2 can only absorb ultra-violet light, or about 4%-5% of the total sunlight energy[5-6], therefore there is a strong initiative to find more efficient catalysts. Hematite (α-Fe_2O_3) is considered a good alternative[7-9] to TiO_2 because of its narrower band-gap, high stability, non-toxicity, and low cost. Indeed, hematite-based nanostructures has recently been found[9] to exhibit outstanding de-NO_x abilities, with both the NO conversion efficiency and selectivity comparable or superior than commercial TiO_2 catalysts. To further improve the catalytic efficiency of hematite, detailed knowledge on its PCO mechanism is essential. The adsorption of NO molecules on the hematite surface is a key step in the PCO process, however some of its main features remain unclear, calling for further investigations.

Computer simulations based on density functional theory (DFT) is a powerful method and in principle well-suited to determine the atomistic adsorption properties[10-15], yet for the NO-hematite system existing reports are conflicting and inconclusive. Song et al.[16] conducted DFT simulations using the Perdew-Burke-Ernzerhof (PBE) exchange-correlation functional[17]. They found that stable chemisorption took place only at the surface Fe sites (denoted as Fe^*) with an adsorption energy of −1.31 eV. In contrast, Li et al.[18] included dispersion corrections (PBE vdw) and determined the adsorption energy as −4.08 eV. Such a large difference is surprising and its origin remains unclear. Moreover, both adsorption energies are quite high, indicating that NO can easily adsorb on the α-Fe_2O_3 surface. This seems in conflict with experimental observations[7,9] where no infrared signals from adsorbed NO molecules were detected when the illumination was off and the NO concentration was low (1×10^{-7}). Note α-Fe_2O_3 is a typical transition metal oxide where the d-electrons

of iron atoms exhibit strong correlations. For such systems the PBE or PBE vdw methods may not be suitable and more advanced techniques such as the PBE+U[19] or hybrid functionals[20] are needed.

Here we use the PBE + U method with dispersion corrections (vdw) to study NO adsorption on the α-Fe_2O_3 (0001) surface. The effects of Hubbard U and vdw were carefully delineated. The microscopic bonding mechanism was determined by analyzing the partial density of states (pdos) and charge density differences before and after NO adsorption. Finally, we applied the Langmuir formula from statistical mechanics to predict the equilibrium coverage as a function of NO concentration in the air.

1 Computational details

Calculations were performed using the plane-wave pseudopotential method as implemented in the open-source QUANTUM-ESPRESSO package[21]. To avoid uncertainties associated with semi-core electrons, we use an ultrasoft pseudopotential[22] with 16 valence electrons ($3s^2 3p^6 3d^6 4s^2$) to describe Fe, N and O were described using ultrasoft pseudopotentials with $2s^2 2p^3$ and $2s^2 2p^4$ valence electrons, respectively. Previous studies have long established that physical properties of hematite are best described by the PBE+U method with $U = 4.2$ eV[23-27], thus we adopt the same U value here. NO is a polar molecule and dipole-dipole interactions may substantially affect its adsorption properties. However such dipole interactions were absent in the standard PBE functional, thus a semi-empirical dispersion correction (vdw)[28] was added to the simulation. The energy cutoff of the plane-wave basis was set to 40 Ry, and the Brillouin zone sampling was conducted at 4×4×2 for the hematite bulk, and 4×4×1 for the slab. With these settings the adsorption energies were converged within 0.01 eV. To ensure the reliability of the calculations, a tight energy convergence criterion (10^{-8} Ry) was set for the electron self-consistent field (scf) calculations. Ionic relaxations were performed until every force component on the atoms was less than 0.2 mRy/bohr (50 meV/nm).

α-Fe_2O_3 maintains a R-3c, corundum structure and is anti-ferromagnetic along the c-axis. Figure 1 shows the slab supercell we are using, where yellow and white arrows distinguish the spin-up and spin-down iron atoms. The surface corresponds to the Fe-O_3-Fe termination, which has been identified as thermodynamically most stable[19,24] at ambient conditions. The slabs were separated by a 24 Å (1 Å = 0.1 nm) vacuum layer so as to minimize their interactions. To delineate the effect of +U and vdw, structural relaxations were performed with four different settings: PBE, PBE vdw, PBE+U, and PBE+U vdw. During the structural relaxation, the atoms in the middle three layers were fixed at their bulk positions, whereas all other atoms were allowed to move.

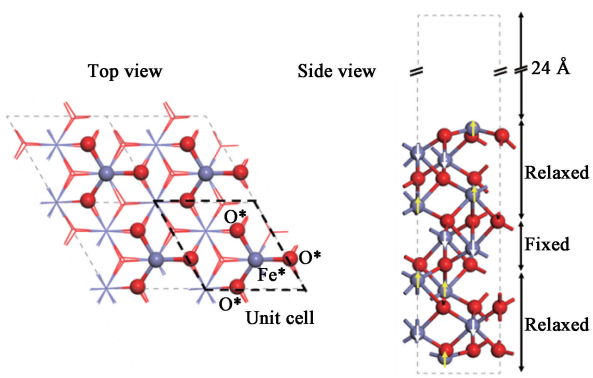

Fig. 1　Schematic diagram of α-Fe_2O_3 (0001) crystal surface

Once structural relaxations were completed, we evaluated the adsorption energy E_{ad} as follows

$$E_{ad} = E_{m+s} - (E_m + E_s), \qquad (1)$$

where E_{m+s}, E_m, and E_s are the energies of the adsorbed system, isolated molecule, and the slab, respectively. A negative E_{ad} indicates the adsorption is exothermic: the greater the absolute value of E_{ad}, the more stable the adsorbed configuration.

To understand the effect of coverage on the adsorption, we first performed the simulation in the 1×1 supercell (100% monolayer coverage), then repeated the simulation in the 2×2 supercell (25% monolayer coverage). The resulting adsorption geometries and energies are nearly identical. In fact, as the distance between adjacent surface Fe*

atoms are more than 5 Å, the interactions among adsorbates are small even at full coverage.

2 Results and discussion

2.1 Adsorption geometries and energies

Prior studies have identified that the most stable NO adsorption configuration as the N atom pointing downwards near vertically to a surface Fe^* atom[16,18], with the N-Fe^* bond length about 1.7 Å. We took this configuration as the initial coordinates and performed structure relaxations under four different settings: PBE, PBE vdw, PBE+U and PBE+U vdw. The resulting adsorption geometries are shown in Fig. 2. Comparisons with prior studies are listed in Table 1. Our PBE results agree very well with those of Song et al.[16], whereas our PBE vdw results differ substantially with Li et al.[18] The adsorption energies of PBE and PBE vdw from our calculations differ by ~0.2 eV, in accordance with the typical range of van der Waals energies[28]. By contrast, the contribution the van der Waals interaction would be 2.77 eV if the adsorption energy of PBE vdw is indeed −4.08 eV[18]. Such a large van der Waals contribution is unreasonable as it exceeds the bond strengths of many covalent bonds. The PBE vdw results obtained from this study is consistent with those of PBE and should be more reliable.

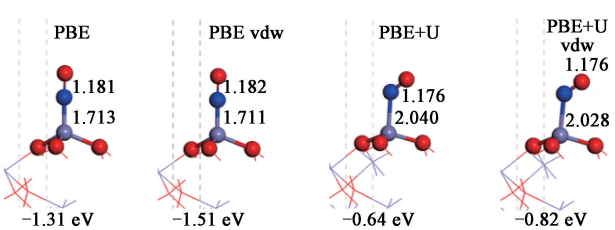

Fig. 2 Adsorption geometries of NO on hematite (0001) surface predicted with four different settings

More importantly, we find that the addition of a Hubbard U term in the DFT Hamiltonic affects strongly the adsorption properties of NO on hematite. Once the U is turned on, the N-Fe^* bond length gets elongated by as much as 0.3 Å. The inclination of the NO molecule also changes substantially, from nearly vertical to the surface (∠O-N-Fe^* = 170°) to an O-N-Fe^* angle of about 125°. The adsorption energy decreases by ~50%, from −1.31 eV to −0.64 eV. This trend is unaffected by the inclusion of dispersion correction (vdw), whose overall effect is to increase the adsorption energy by ~0.18 eV while causes little changes in the adsorption geometries. It has been known that for transition metal oxides[29] the DFT+U can predict adsorption properties different from those of standard DFT. However to our knowledge this is yet to be reported for NO-hematite. In fact, in our previous study on the SO_2 adsorption on the hematite surface[27], the adsorption energy was found to be nearly independent of U, thus it is surprising to see NO behaves so differently.

Table 1 Adsorption properties of NO on α-Fe_2O_3(0001) surface

Method	E_{ad}/eV	$d_{N\text{-}O}$/Å	$d_{N\text{-}Fe^*}$/Å	∠O-N-Fe^*/(°)
PBE[a]	−1.31	1.185	1.738	
PBE vdw[b]	−4.08	1.170	1.680	179.7
PBE	−1.31	1.181	1.713	169.7
PBE vdw	−1.51	1.182	1.711	170.1
PBE+U	−0.64	1.176	2.040	125.4
PBE+U vdw	−0.82	1.176	2.028	126.1

[a]Ref. [16].
[b]Ref. [18].

2.2 Electronic structures

To understand why the addition of Hubbard U affects the adsorption properties of NO, and to gain physical insights on the bonding mechanism, we now examine the electronic structure of the system before and after adsorption, as shown in Fig. 3. A NO molecule has two types of molecular orbitals: those aligned head-to-head (σ_z) or side-by-side (π_x and π_y) along the N-O axis. As the total number of electrons in NO is odd, there is an unpaired electron occupying the higher energy anti-bonding π-orbital (denoted as π_x^* in Fig. 3). Upon adsorption, these orbitals tends to mix with those from the surface atom (Fe^*) of similar energies, forming new chemical bonds. In the PBE case where the iron 3d orbitals are dispersive, such hybridizations take place in both the bonding and the antibonding orbitals (Fig. 3(a), lower panel): the σ_z(π_x and π_y) bonding orbital hybrids with d_{z^2}(d_{zx} and d_{zy}),

whereas the π_x^* and π_y^* antibonding orbitals hybrid with d_{zx} and d_{zy}. In the PBE+U case, the iron 3 d orbitals are squeezed to lower energies (Fig. 3 (b), upper panel) and hybridization takes place only in the bonding orbitals (Fig. 3 (b), lower panel). The different extents of hybridization explain why the adsorption energy predicted by PBE+U is lower than PBE. Interestingly, for the O_2 adsorption on the hematite (0001) surface the adsorption energy predicted by PBE + U[30] (−0.33 eV) is also lower than that of PBE[31] (−0.5 to −1.0 eV, depending on the tilting direction). This may be related to the fact that an O_2 molecule in its triplet ground state has two unpaired π^* electrons, similar to NO. Conversely, the SO_2 molecule does not have unpaired electrons and is therefore less sensitive to U[27]. Moreover, for the PBE case the rotational symmetry along the z-axis is preserved in the orbital hybridization. Accordingly, the predicted adsorption geometry has the NO molecule hanging near perpendicularly at the top of the Fe^* atom. By contrast, the rotational symmetry is broken in the PBE+U case, as the σ, π and d orbitals are all mixed in the energy range −5.5 eV to −7 eV (Fig. 3(b), lower panel), in consistent with the fact that the Fe^*-N-O bond angle is 125°.

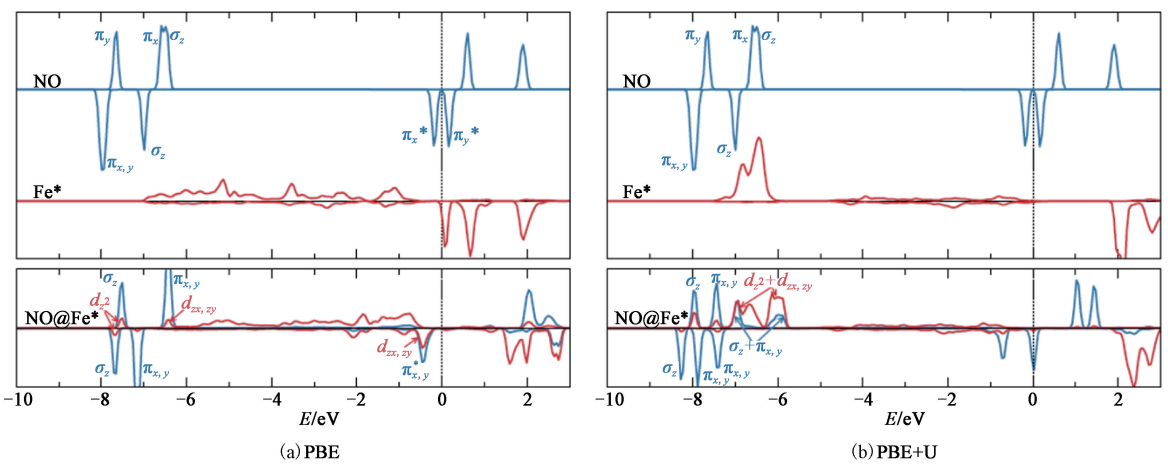

Fig. 3　Partial density of states of the NO molecule and the surface Fe atom (Fe^*) before (upper panel) and after (lower panel) adsorption using (a) PBE and (b) PBE+U

Further insights can be obtained by examining the charge density difference with and without Hubbard-like U correction, as shown in Fig. 4. Upon adsorption, significant charge accumulations take place in the region between the N and the Fe^* atoms, indicating that the adsorption is mainly driven by forming new covalent bonds rather than charge transfer reactions such as $Fe^{3+} + NO = NO^+ + Fe^{2+}$. Indeed, the integrated charge difference in the region occupied by the NO molecule is less than 0.01e. By contrast, the integrated charge difference in the region between the N and the Fe^* atoms is 0.18 e (PBE) and 0.08 e (PBE+U), respectively. The less covalent charge predicted in the PBE+U calculation is consistent with its smaller adsorption energy.

We now consider the effect of dispersion correction (vdw) on the electronic structures. This semi-empirical correction is not involved in the scf cycles to determine the electronic ground state, yet it can exert an indirect influence on the electronic structure by changing the final relaxed coordinates. As the changes in the relaxed coordinates are small (see Table 1), we find the associated changes in the electronic structure are minor. Still, as dipole-dipole interactions are present in real systems, we use the adsorption properties evaluated with vdw to compare with experiments.

2.3　Equilibrium coverage

We now apply the information obtained in prior sections to calculate the equilibrium coverage of NO on hematite. Assume a mono-layer adsorption where

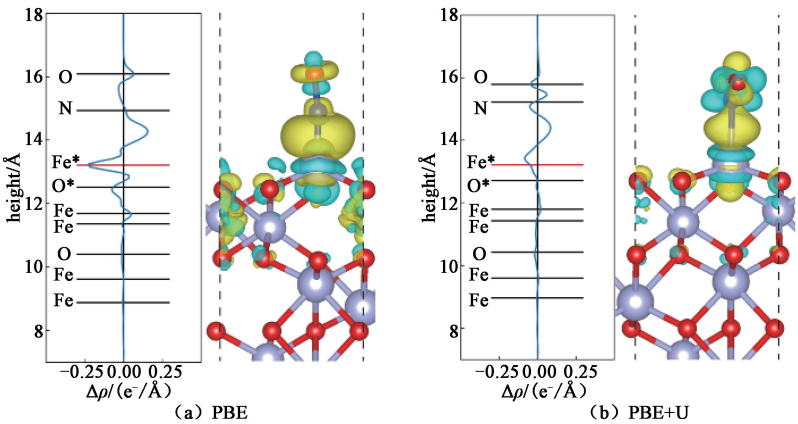

The iso-surface value is ±0.02 e/Å^3.

Fig. 4 Charge density difference after adsorption

the adsorption configuration at each adsorption site is identical and the adsorbates do not interact, the thermal equilibrium coverage of the adsorbed molecule can be expressed in terms of the Langmuir formula[32] as

$$\Theta(P,T)=\frac{P}{P+P^0\exp(\frac{G^0_{ad}}{k_BT})}, \qquad (2)$$

where P denotes the partial pressure of the adsorbate in the gas phase, P^0 is the standard atmospheric pressure (1 atm = 10^5 Pa), G^0_{ad} is the adsorption free energy at standard condition. As entropic effects are insignificant for the condensed phase, G^0_{ad} can be well approximated as

$$G^0_{ad}=E_{ad}-\Delta G_m(T,P^0), \qquad (3)$$

where $\Delta G_m(T,P^0)$ is the Gibbs energy change of the gas molecule from 0 K to T at the standard atmospheric pressure. For NO it equals −0.56 eV at 298.15 K[33]. The resulting $\Theta(P)$ are shown in Fig. 5. As the E_{ad} from PBE vdw is high (−1.51 eV), substantial amount of NO will be adsorbed on the surface even when the NO partial pressure is as low as 10^{-12} Pa. In fact, a full coverage is achieved when $P>10^{-9}$ Pa. By contrast, the E_{ad} from PBE+U vdw is low (−0.82 eV) and a full coverage can be achieved only when $P>100$ Pa. In the experiments[7,9], no infrared signal from the adsorbed NO molecules were observed when the light was off and the NO concentration is 1×10^{-7} (P = 0.01 Pa), indicating that the amount of adsorbates is scarce under such conditions. By contrast, distinct infrared signals from the adsorbed NO molecules were detected when the NO partial pressures were greater than 5 Torr (667 Pa)[34]. These observations are consistent with the $\Theta(P)$ predicted by PBE+U vdw while in conflict with that of PBE vdw. We therefore conclude that including the Hubbard U provides a more accurate description of the system.

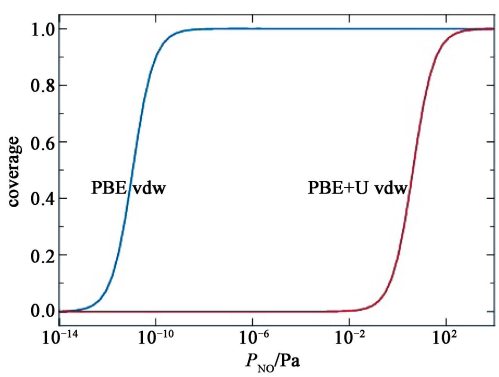

Fig. 5 Equilibrium Coverage of NO molecule on the Hematite (0001) surface at 298.15 K

The above analysis considers only one type of gas molecule (NO) adsorbing on the hematite surface. This is appropriate when the illumination is off. When the illumination is on, electron-hole pairs will be generated at the hematite surface. These electron-hole pairs will interact with the O_2, H_2O molecules in the air and convert NO into thermodynamically more stable compounds such as NO_3. The formation of NO_3 is crucial in trapping significant amount of NO molecules on the hematite surface, otherwise for typical NO concentrations in the atmosphere, the number of adsorbed NO

molecules would be scarce. The exact mechanism of this de-NO_x process, as well as how to use this mechanism to further improve the catalytic efficiency of hematite, will be a focus for future research.

3 Conclusions

We have studied the adsorption of NO molecules on the hematite (0001) surface using DFT. We found that the inclusion of a Hubbard term in the DFT Hamiltonian strongly affects the NO adsorption geometries and energies. The smaller adsorption energies predicted with + U yield equilibrium coverages that are more consistent with experimental observations. As this U-dependence is related to the unpaired electron of the NO molecule, we anticipate similar behavior in other molecules such as NO_2, which also possess lone electrons. In contrast, the effect of dispersion correction is not as dramatic as previous studies may indicate, as the adsorption geometries and electronic structures with or without the vdw correction are nearly identical. This work clarifies the mechanism of the NO adsorption, and paves the way for further work to fully understand the de-NO_x process on the hematite surface.

References

[1] Choo G H, Seo J, Yoon J, et al. Analysis of long-term (2005-2018) trends in tropospheric NO_2 percentiles over Northeast Asia [J]. Atmospheric Pollution Research, 2020, 11(8): 1429-1440. DOI:10.1016/j.apr.2020.05.012.

[2] Yu Y, Liu H R. Economic growth, industrial structure and nitrogen oxide emissions reduction and prediction in China [J]. Atmospheric Pollution Research, 2020, 11(7): 1042-1050. DOI:10.1016/j.apr.2020.03.011.

[3] Ren H J, Koshy P, Chen W F, et al. Photocatalytic materials and technologies for air purification[J]. Journal of Hazardous Materials, 2017, 325: 340-366. DOI: 10.1016/j.jhazmat.2016.08.072.

[4] Wang X C, Anpo M, Fu X Z. Current developments in photocatalysis and photocatalytic materials [M]. Amsterdam: Elsevier, 2020: 1-6. DOI: 10.1016/b978-0-12-819000-5.00001-1.

[5] Chen H H, Nanayakkara C E, Grassian V H. Titanium dioxide photocatalysis in atmospheric chemistry [J]. Chemical Reviews, 2012, 112(11): 5919-5948. DOI: 10.1021/cr3002092.

[6] Pelaez M, Nolan N T, Pillai S C, et al. A review on the visible light active titanium dioxide photocatalysts for environmental applications [J]. Applied Catalysis B: Environmental, 2012, 125: 331-349. DOI: 10.1016/j.apcatb.2012.05.036.

[7] Sugrañez R, Balbuena J, Cruz-Yusta M, et al. Efficient behaviour of hematite towards the photocatalytic degradation of NO_x gases [J]. Applied Catalysis B: Environmental, 2015, 165: 529-536. DOI:10.1016/j.apcatb.2014.10.025.

[8] Balbuena J, Cruz-Yusta M, Pastor A, et al. A-Fe_2O_3/SiO_2 composites for the enhanced photocatalytic NO oxidation[J]. Journal of Alloys and Compounds, 2018, 735: 1553-1561. DOI:10.1016/j.jallcom.2017.11.259.

[9] Balbuena J, Cruz-Yusta M, Cuevas A L, et al. Hematite porous architectures as enhanced air purification photocatalyst [J]. Journal of Alloys and Compounds, 2019, 797: 166-173. DOI:10.1016/j.jallcom.2019.05.113.

[10] Rodriguez J A, Jirsak T, Liu G, et al. Chemistry of NO_2 on oxide surfaces: formation of NO_3 on TiO_2(110) and NO_2↔O vacancy interactions [J]. Journal of the American Chemical Society, 2001, 123(39): 9597-9605. DOI: 10.1021/ja011131i.

[11] Liu Z M, Ma L L, Junaid A S M. NO and NO_2 adsorption on Al_2O_3 and Ga modified Al_2O_3 surfaces: a density functional theory study [J]. The Journal of Physical Chemistry C, 2010, 114(10): 4445-4450. DOI:10.1021/jp907925w.

[12] Yu Y Y, Diebold U, Gong X Q. NO adsorption and diffusion on hydroxylated rutile TiO_2(110) [J]. Physical Chemistry Chemical Physics: PCCP, 2015, 17(40): 26594-26598. DOI:10.1039/c5cp04584c.

[13] Xie X Y, Wang Q, Fang W H, et al. DFT study on reaction mechanism of nitric oxide to ammonia and water on a hydroxylated rutile TiO_2(110) surface [J]. The Journal of Physical Chemistry C, 2017, 121(30): 16373-16380. DOI: 10.1021/acs.jpcc.7b04811.

[14] Pan J, Hu Z B. Simulation of CTAB bilayer adsorbed on Au(100), Au(110), and Au(111) surfaces: structure stability and dynamic properties [J]. Journal of University of Chinese Academy of Sciences, 2017, 34(1): 38-49. DOI:10.7523/j.issn.2095-6134.2017.01.006.

[15] Fang L C, Hao K R, Yan Q B, et al. Adsorption and migration of Li-ion in layered $SnSe_2$: a first principle study [J]. Journal of University of Chinese Academy of Sciences, 2018, 35(6): 735-742. DOI:10.7523/j.issn.2095-6134.2018.06.004.

[16] Song Z J, Wang B, Yu J, et al. Density functional study on the heterogeneous oxidation of NO over α-Fe_2O_3 catalyst by H_2O_2: effect of oxygen vacancy [J]. Applied Surface Science, 2017, 413: 292-301. DOI: 10.1016/j.apsusc.2017.04.011.

[17] Perdew J P, Burke K, Ernzerhof M. Generalized gradient approximation made simple [J]. Physical Review Letters,

1996, 77(18): 3865-3868. DOI:10.1103/PhysRevLett.77.3865.

[18] Li F F, Shi C M, Wang X F, et al. The important role of oxygen defect for NO gas-sensing behavior of α-Fe_2O_3(001) surface: predicted by density functional theory [J]. Computational Materials Science, 2018, 146: 1-8. DOI:10.1016/j.commatsci.2017.12.065.

[19] Rohrbach A, Hafner J, Kresse G. Ab initio study of the (0001) surfaces of hematite and chromia: influence of strong electronic correlations[J]. Physcial Review B, 2004, 70(12): 1-17. DOI:10.1103/physrevb.70.125426.

[20] Von Rudorff G F, Jakobsen R, Rosso K M, et al. Hematite (001)-liquid water interface from hybrid density functional-based molecular dynamics [J]. Journal of Physics: Condensed Matter, 2016, 28(39): 394001. DOI:10.1088/0953-8984/28/39/394001.

[21] Giannozzi P, Baroni S, Bonini N, et al. QUANTUM ESPRESSO: a modular and open-source software project for quantum simulations of materials [J]. Journal of Physics: Condensed Matter, 2009, 21(39): 395502. DOI:10.1088/0953-8984/21/39/395502.

[22] Vanderbilt D. Soft self-consistent pseudopotentials in a generalized eigenvalue formalism [J]. Physical Review B: Condensed Matter, 1990, 41(1): 7892-7895. DOI: 10.1103/physrevb.41.7892.

[23] Liao P L, Keith J A, Carter E A. Water oxidation on pure and doped hematite (0001) surfaces: prediction of Co and Ni as effective dopants for electrocatalysis [J]. Journal of the American Chemical Society, 2012, 134(32): 13296-13309. DOI:10.1021/ja301567f.

[24] Nguyen M T, Seriani N, Gebauer R. Water adsorption and dissociation on α-Fe_2O_3(0001): PBE+U calculations[J]. The Journal of Chemical Physics, 2013, 138(19):194709. DOI:10.1063/1.4804999.

[25] Nguyen M T, Seriani N, Piccinin S, et al. Photo-driven oxidation of water on α-Fe_2O_3 surfaces: an ab initio study [J]. The Journal of Chemical Physics, 2014, 140(6): 064703. DOI:10.1063/1.4865103.

[26] Nguyen M T, Piccinin S, Seriani N, et al. Photo-oxidation of water on defective hematite (0001) [J]. ACS Catalysis, 2015, 5(2): 715-721. DOI:10.1021/cs5017326.

[27] Zhao H L, Sheng X, Fabris S, et al. Heterogeneous reactions of SO_2 on the hematite(0001) surface [J]. The Journal of Chemical Physics, 2018, 149(19): 194703. DOI:10.1063/1.5037847.

[28] Grimme S. Semiempirical GGA-type density functional constructed with a long-range dispersion correction [J]. Journal of Computational Chemistry, 2006, 27(15): 1787-1799. DOI:10.1002/jcc.20495.

[29] Rohrbach A, Hafner J. Molecular adsorption of NO on NiO (100): DFT and DFT+U calculations [J]. Physical Review B, 2005, 71(4): 1-7. DOI:10.1103/physrevb.71.045405.

[30] Souvi S M O, Badawi M, Paul J F, et al. A DFT study of the hematite surface state in the presence of H_2, H_2O and O_2 [J]. Surface Science, 2013, 610: 7-15. DOI:10.1016/j.susc.2021.12.012.

[31] Bergermayer W, Schweiger H, Wimmer E. Ab initio thermodynamics of oxide surfaces: O_2 on Fe_2O_3(0001) [J]. Physical Review B, 2004, 69(19): 195409. DOI:10.1103/physrevb.69.195409.

[32] Atkins P, Paula J. Physical chemistry[M]. Oxford: Oxford University Press, 2010.

[33] National Institute of Standards and Technology, U.S. Department of Commerce. NIST standard reference database 13. NIST-JANAF thermochemical tables [EB/OL]. (2019-06-11) [2020-05-08]. https://janaf.nist.gov/.

[34] Busca G, Lorenzelli V. Infrared study of the adsorption of nitrogen dioxide, nitric oxide and nitrous oxide on hematite [J]. Journal of Catalysis, 1981, 72(2): 303-313. DOI:10.1016/0021-9517(81)90013-0.